Flow-Induced Deformation and Desorption of Adsorbed Polymers

Iwao Soga† and Steve Granick*

Department of Materials Science and Engineering, University of Illinois, Urbana, Illinois 61801

Received January 7, 1998. In Final Form: May 18, 1998

The influence of shear flow of solvent past poly(methyl methacrylate) chains adsorbed onto germanium oxide from dilute carbon tetrachloride solution (a near-θ solvent) was studied at shear rates from 0 to 4 $\times 10^4$ s^{-1} with the new apparatus described in this paper. Both the adsorbed amount and the flow-induced surface orientation (surface dichroism) were measured. The method involved measurements of infrared spectroscopy in attenuated total reflection (FTIR-ATR) using a hemispherical ATR crystal whose position with respect to the incident infrared source was rotated by 90° during the experiment in order to measure infrared absorbance in orthogonal directions. shear flow appeared to flatten the adsorbed PMMA layer relative to the surface. However, alignment of the polymer orientation in the direction of flow was found to be small. This suggests that shear-induced desorption (controlled by stress) and relaxation in response to deformation within the adsorbed layer (controlled by time) may be largely independent.

Introduction

When polymers meet an attractive interface, they adsorb. Therefore, since polymers are so useful and so ubiquitous, polymer adsorption underlies key technologies in diverse applications. The applications range from filled polymers and paints to food products, pharmaceuticals, and lubrication of biological joints. Most of the scientific work in this area has focused upon understanding basic properties such as the adsorbed amount, layer thickness, and segmental density distribution. This body of accomplishment now provides a sophisticated view of adsorbed polymer layers under equilibrated conditions.[1−3] Here, we focus instead on adsorbed polymers under situations deliberately far from equilibrium, where the adsorbed state competes with an externally applied field such as a shear field.

Some shear force or other flow field is commonly applied in many practical situations.[4,5] As one practical example, a convection process is required to achieve efficient mixing when a polymer solution or melt is introduced to a solid surface. The speed of this process may be high enough to disturb a polymer's shape as the adsorbed layer forms. Adsorbed polymer layers are thus exposed to strong mechanical shear and high-speed flow conditions during common mixing and dispersion processes. To understand real applications, it is important to understand the effects of flow fields on polymer adsorption.

Relatively few prior studies of polymer adsorption have been performed under flow.[6−18] One experimental approach is based on observing a flow rate reduction owing to the layer thickness of adsorbed polymers during flow through capillary tubes or porous media. This change of effective hydrodynamic thickness has been measured for polymers of high molecular weight in both good and theta solvents, and thickness changes as a function of flow rate have been reported. A second approach is based on using ellipsometry to study polystyrene adsorption onto a single chromium plate. Both the adsorbed mass and the average layer thickness are measured by this method. Desorption at high shear rate, accompanied by reduction of the layer thickness, has been observed. Theoretical work has also been performed, mainly for the effects of flow fields on isolated grafted chains.[19,20] Recently computer simulation was used to study similar questions.[21] It is immediately apparent that, depending on the technique employed, experimental measurements of the effective hydrodynamic thickness under flow conditions vary not only in magnitude but also in sign. It is clear that a basic understanding of surface properties demands direct knowledge of surface molecular orientation.

Here we use Fourier transform infrared spectroscopy in attenuated total reflection (FTIR-ATR)[22,23] to measure polymer adsorption under flow. One of the advantages of this technique is that adsorption of several discrete components within a mixture can be measured indepen-

* To whom correspondence may be addressed. E-mail: sgranick@uiuc.edu. Phone: 217-333-5720. Fax: 217-323-2736.

† Permanent address: Mitsubishi Chemical Corporation, Yokohama, Kanagawa 227, Japan.

(1) Fleer, G. J.; Cohen Stuart, M. A.; Scheutjens, J. M. H. M.; Cosgrove, T.; Vincent, B. *Polymers at Interfaces*; Chapman and Hall: New York, 1993.

(2) Kawaguchi, M.; Takahashi, A. *Adv. Colloid Interface Sci.* **1992**, *37*, 219.

(3) de Gennes, P.-G. *Adv. Colloid Interface Sci.* **1992**, *27*, 189.

(4) Larson, R. G. *Rheol. Acta* **1992**, *31*, 497.

(5) Patton, T. C. *Paint Flow and Pigment Disperson*; John Wiley and Sons: New York, 1979.

(6) Hikmet, R. A. M.; Narh, K. A.; Barham, P. J.; Keller, A. *Prog. Colloid Polym. Sci.* **1985**, *71*, 32.

(7) Keller, A.; Odell, J. A. *Colloid Polym. Sci.* **1985**, *263*, 181.

(8) Narh, K. A.; Barham, P. J.; Hikmet. R. A. M.; Keller, A. *Colloid Polym. Sci.* **1986**, *264*, 507.

(9) Lee, J.-J.; Fuller, G. G. *J. Colloid Interface Sci.* **1985**, *103*, 569.

(10) Lee, J.-J.; Fuller, G. G. *Macromolecules* **1984**, *17*, 375.

(11) Besio, G. J.; Prud'homme, R. K.; Benziger, J. B. *Macromolecules* **1988**, *21*, 1070.

(12) McGlinn, T. C.; Kuzmenka, D. J.; Granick, S. *Phys. Rev. Lett.* **1988**, *60*, 805.

(13) Chin, S.; Hoagland, D. A. *Macromolecules* **1991**, *24*, 1876.

(14) Parnas, R. S.; Cohen, Y. *Macromolecules* **1991**, *24*, 4646.

(15) Cohen, Y. *Macromolecules* **1988**, *21*, 494.

(16) Gramain, Ph.; Myard, Ph. *Macromolecules* **1981**, *14*, 180.

(17) Bagassi, M.; Chauveteau, G.; Lecourtier, J.; Englert, J.; Tirrell, M. *Macromolecules* **1989**, *22*, 262.

(18) Frantz, P.; Perry, D.; Granick, S. *Colloids Surf.* **1994**, *86*, 295.

(19) Aubouy, M.; Harden, J. L.; Cates, M. E. *J. Phys. II* **1996**, *6*, 969.

(20) Halioglu, T.; Bahar, I.; Erman, B. *J. Chem. Phys.* **1996**, *105*, 2919.

(21) Grest, G. S., in press.

(22) Johnson, H. E.; Granick, S. *Macromolecules* **1990**, *23*, 3367.

(23) Frantz, P.; Granick, S. *Macromolecules* **1995**, *28*, 6915.

S0743-7463(98)00040-7 CCC: $15.00
Published on Web 06/25/1998

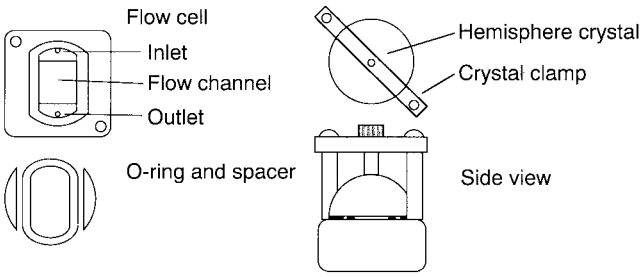

Figure 1. Schematic illustration of the flow cell. Measurements were made, using Fourier transform infrared spectroscopy in attenuated total reflection (FTIR-ATR), of polymer flow past a hemispherical ATR crystal to which the polymer adsorbed. The top views are separated into three parts to avoid overlap. The O-ring and spacer, shown in the second panel from top, were placed onto a metal surface, and the hemispherical crystal was placed onto this and secured by clamps. The side view shows all parts placed together.

dently at the same time. This provides more molecular detail than simply measuring the total amount adsorbed. A second advantage is that, if polarized light is employed, the orientation of specific functional groups with respect to the surface can be measured. Previously, using these methods during adsorption from stagnant solution, we measured the infrared dichroism of carbonyl groups of adsorbed poly(methyl methacrylate) (PMMA)[23,24] and inferred the orientational distribution; however, a limitation of the data analysis was that orientation in a preferred direction of the plane of the solid substrate surface could not be measured.

With the new flow cell described in this paper, FTIR-ATR measurements were made using a hemispherical ATR crystal whose position with respect to the incident infrared source was rotated 90° during the experiment in order to measure directly the infrared absorbance in orthogonal directions. This, we will show in this paper, allows one to determine not only the total adsorption but also the flow-induced segmental alignment. The flow-induced orientation of the polymer backbone under flow can be inferred, provided that the angle between the polymer backbone and specific functional groups that are pendant to it is known.

Capabilities of this new flow cell are illustrated by experiments using poly(methyl methacrylate) (PMMA) adsorbed onto germanium from carbon tetrachloride solution and subjected to shear rates up to 3×10^4 s^{-1}. This polymer was selected mainly because of the intense infrared absorptivity of the carbonyl group. An additional reason for selection was that aging of the adsorbed layer, studied by us previously for a weakly adsorbed polymer, polystyrene,[25] is so slow for PMMA that it did not influence the results during the time period (several h) of these experiments, thus allowing us to separate that effect from direct measurements of the consequences of shear flow.

Experimental Section

Flow Cell. Figure 1 shows a schematic drawing of the flow cell. Its three elements consist of a steel flow channel, O-ring and spacer, a hemispherical ATR crystal, and clamps. Flow is bounded on one horizontal side by the ATR crystal and on the other horizontal side by metal (stainless steel). The space between them is sealed by the Teflon-coated rubber O-ring that sits within a groove cut into the metal flow channel. The gap thickness of the flow channel can be varied by the choice of the spacer thickness. The assembled cell is placed into a cell holder, equipped with temperature control, that is mounted onto a motorized rotator in order to switch optical paths in orthogonal directions.

Inlet and outlet holes are placed at opposite sides of the flow channel and connected to a solvent reservoir and a pump (Master Flex, from Micropump, Inc.) via fittings and Teflon tubes. To produce laminar flow over the ATR crystal, the volume is relatively large and deep on the inlet and outlet sides, and relatively small and thin over the ATR crystal itself.

To minimize the possible influence of edge and entrance influences on the spectroscopic measurements, the size of the flow channel (~10 mm long and 11 mm wide) was chosen to be larger than that of the IR beam spot (estimated to be <5 mm in diameter).

The apparent velocity gradient was calculated, assuming a fully developed velocity profile, as

$$\gamma = 6Q/WB^2 \qquad (1)$$

where Q is the volume flow rate, W is the channel width, and B is the channel thickness. The channel was not precisely rectangular, however; though half the thickness of the cylindrical O-ring ($^3/_{32}$ in. diameter) sat below the flow space, the upper half protruded from the grooved metal support. Approximating this curvature as a triangular line, the reduction of the effective volume flow rate of a Newtonian fluid can be calculated.[26] In the studies reported below, the gap was 0.39 mm, and the estimated correction to eq 1 was less than 5%.

In the experiments reported below, the shear rate ranged between 0 and 3×10^4 s^{-1} as the pump rate of solvent was varied from 0 to 600 mL min^{-1}, giving a residence time of solvent in the flow cell as short as 1 s.

ATR Spectroscopy. Infrared spectra were collected using a Bio-Rad FTS6000 Fourier transform infrared spectrometer (FTIR). A purged sample compartment, external to the FTIR instrument itself, was built to house the flow cell described in the previous section. The IR beam was directed onto the focal point of the ATR hemispherical Ge crystal using an off-axial parabolic mirror at incident angle 45°. Polarization was accomplished using a KRS polarizer held within a motorized actuator. Signals were detected using a liquid nitrogen cooled mercury−cadmium−telluride (MCT) detector.

Figure 2 shows a schematic diagram of the ATR optical geometry. The IR beam propagated within the Ge crystal was totally reflected at the crystal surface and produced an evanescent

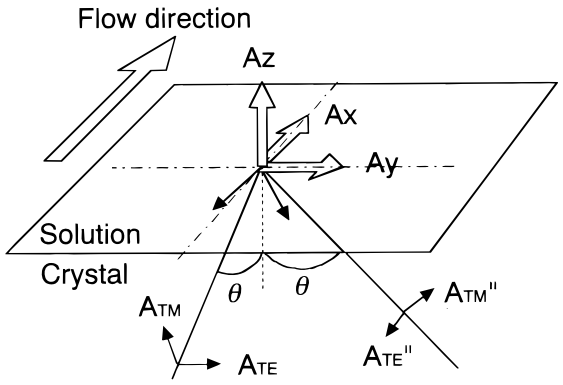

Figure 2. Illustration of the coordinate system used in the data analysis. Here the Cartesian coordinate x indicates the direction of shear flow, y is also in the plane of the surface but is perpendicular to the flow, and z is normal to the surface. The IR light traveled from the crystal side (lower side in the figure) and experienced total reflection at the solid surface. Polarized ATR intensities were measured parallel (A_{TM}, A_{TE}) and perpendicular ($A_{TM''}$, $A_{TE''}$) to the flow direction. Subscripts denote that, in TM mode, the electric field was parallel to the incident plane and, in the TE mode, was normal to the incident plane. These four absorbances are related, by eqs 2−5, to the adsorptions of Cartesian elements A_x, A_y, and A_z at the solid−liquid interface.

(24) Enriquez, E.; Schneider, H. M.; Granick, S. *J. Polym. Sci., Polym. Phys. Ed.* **1995**, *33*, 2429.

(25) Frantz, P.; Granick, S. *Phys. Rev. Lett.* **1991**, *66*, 899.

(26) Tucker, C. private communication.

electric field on the side of lesser refractive index. Figure 2 illustrates that the IR beam could be absorbed with absorbances A_x, A_y, and A_z in the Cartesian directions. We use the convention that x and y were in the plane of the surface and that z was perpendicular to it.

By rotating the flow cell 90° with respect to the incident IR beam, the IR beam was alternately directed parallel or perpendicular to the flow direction. In both cases it was polarized in either the p direction (parallel to the plane of incidence) or the s direction (perpendicular to the plane of incidence). Absorbances in these two polarizations (A_{TM} and A_{TE}, respectively) were compared. For incidence parallel to the flow direction, absorbances at the crystal surface in the Cartesian axes are related to A_{TM} and A_{TE} by simple formulas[27]

$$A_{TM} = \alpha A_x + \beta A_z \quad (2)$$

$$A_{TE} = \gamma A_y \quad (3)$$

Here α, β, and γ are constants calculated from the known angle of incidence and the known refractive indices of the solvent and the crystal. These equations assume that the real parts of the refractive indices are isotropic and that the imaginary parts are negligibly small. In addition, when the flow cell was rotated 90° so that the incident beam was perpendicular to the flow direction, new quantities $A_{TM''}$ and $A_{TE''}$ were measured. These provide analogous additional relations

$$A_{TM}'' = \alpha A_y + \beta A_z \quad (4)$$

$$A_{TE}'' = \gamma A_x \quad (5)$$

From these four measurements (A_{TM}, A_{TE}, $A_{TM''}$, and $A_{TM''}$) the quantities A_x, A_y, and A_z can be calculated from eqs 2−5.

Samples and Procedure. To enhance the chances of observing flow-induced effects, following previous work[10,11] we chose polymers of high molecular weight. (We also performed trial experiments which confirmed smaller effects when the polymer molecular weight was less.) Atactic poly(methyl methacrylate) (weight-average molecular weight M_w = 2 200 000 g mol^{-1} and ratio of number-average to weight-average molecular weight M_w/M_n = 1.16) was purchased from Polymer Laboratories. Carbon tetrachloride was purchased from Aldrich and used as received. The hemispherical ATR crystal (1 in. diameter) was purchased from Harrick Scientific. Temperature was controlled at 25.0 °C. For PMMA in CCl_4, this is believed to be close to the θ temperature.[12]

Procedures to clean the flow cell and crystal surface by oxygen plasma or UV-ozone treatment were the same as reported previously.[28] This cleaning process produces a reproducibly oxidized surface.[28] Cleaning for the pump was the same as for the flow cell.

Experiments began by circulating CCl_4 through the system. After the unit was stabilized overnight, background spectra of A_{TM}, A_{TE}, $A_{TM''}$, and $A_{TE''}$ were collected. The pure CCl_4 was then replaced by a solution of ∼0.05 mg-mL^{-1} of PMMA in CCL_4, and the solution was made to enter the cell at very low flow rate, ∼1 s^{-1}. (The layers were in-plane homogeneous after deposition, as shown in Figure 4; therefore flow during deposition is unlikely to have affected the experiments.) To ensure a sufficient supply of polymer, the solution was circulated from time to time. The shear rate during the initial adsorption process was small compared to the high shear rates applied later.

After waiting for PMMA to saturate the surface (a rapid process for this sample at this solution concentration), the solution was replaced by pure CCl_4, and the flow rate was increased from 0 to 1.1 × 10^4, to 2.5 × 10^4, to 3.8 × 10^4 s^{-1}, and, finally, back to zero. Equilibration for 1 h was allowed at each stage, during which the system was monitored for possible kinetic changes.

Results and Discussion

Raw Spectra. Figure 3 shows the carbonyl peak of our PMMA sample when it adsorbed onto Ge from dilute CCl_4 in the absence of flow. The four spectra are measured in two orthogonal directions with two orthogonal polarizations.

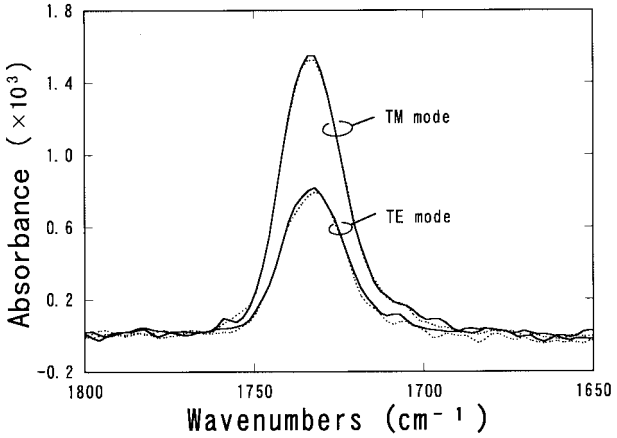

Figure 3. Infrared spectrum of PMMA adsorbed onto Ge from carbon tetrachloride solution from stagnant solution. Solid lines denote spectra taken with incident light parallel to the flow direction (A_{TM}, A_{TE}). Dotted lines denote spectra taken with incident light perpendicular to the flow direction ($A_{TM''}$, $A_{TE''}$). Absorbances in the TM mode are, as expected, nearly twice as large as in the TE mode. Absorbances parallel and perpendicular to the flow direction are nearly equal, meaning that there was no preferential orientation in the flow direction.

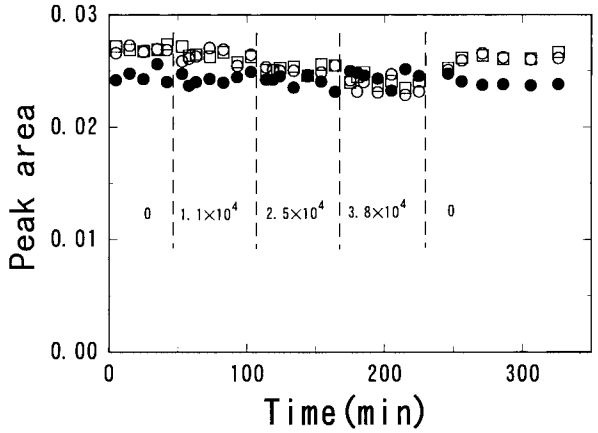

Figure 4. Plot of time evolution of the peak area of the free carbonyl peaks as PMMA adsorbed onto Ge from the carbon tetrachloride solution and was exposed to solvent flows of successively larger magnitude (indicated in the figure with units of s^{-1}). Time zero denotes when the PMMA solution was replaced by pure carbon tetrachloride solvent. The vertical dashed lines denote times when the shear rate was changed. Filled circles denote absorbance in the z direction (normal to the crystal surface). Open circles denote absorbance in the y direction; these data were equal, within the experimental uncertainty, to absorbance in the x direction.

Figure 3 confirms one's expectation of symmetry in the $x-y$ plane in the absence of flow; $A_{TE} = A_{TE''}$ and $A_{TM} = A_{TM''}$. This symmetry must hold on physical grounds. The experimental confirmation shows that, though repeatability has sometimes been a problem in prior measurements that employed hemispherical crystals,[29] rotation of the adsorption cell by 90° could be reliably and reproducibly performed in the present apparatus.

The ratio, $A_{TE}/A_{TM} \approx 1.6$, in Figure 3, is less than $A_{TE}/A_{TM} \approx 2$ expected for a three-dimensionally isotropic sample measured in ATR geometry with the present

(27) Flournoy, P. A.; Schaffers, W. J. *Spectrochim. Acta* **1966**, *22*, 15.
(28) Frantz, P.; Granick, S. *Langmuir* **1992**, *8*, 1176.
(29) Gupta, M. K.; Carlsson, D. J.; Wiles, D. M. *J. Polym. Sci.* **1984**, *22*, 1011.

incident angle of 45°. This indicates a slight preference for the distribution of the carbonyl stretch vibration to be parallel to the surface. Although this C═O group does not lie along the chain backbone, it nonetheless gives some information about the adsorbed layer structure, as we will discuss below.

In Figure 3, one notices that the C═O absorption is asymmetric; it shows a shoulder of excess absorption on the low wavenumber side. This observation is usually ascribed to hydrogen bonding to the surface[30] and can even be used to quantify hydrogen bonding in the bulk.[31] In the bulk, molar absorptivity of the hydrogen-bonded peak is believed to be 50% larger than that for unrestrained vibration.[31] Here, for adsorption onto oxidized Ge, we also observe this sideband. The center of the new peak and its molar absorptivity are not known, however. Therefore, to analyze these data, we chose from spectra measured in solution the center position of the free peak and then fitted the measured spectra to this peak in combination with a second one. Curve-fitting showed this second peak to be symmetric and centered at 1719 cm^{-1}. We suppose this peak to reflect hydrogen bonding to the surface. Attempts to calculate the molar absorptivity of this band by comparison to the integrated absorbance of other vibrational bands were unsuccessful; the estimated molar absorptivity scattered between 60 and 120% of that of the free peak, and the accuracy was low. In the analysis below, we assume the same molar absorptivity as for the unbound polymer, recognizing that the absolute determination will be less accurate than relative changes.

Adsorbed PMMA Subjected to Solvent Flow. In Figure 4, A_x, A_y, and A_z of the PMMA free carbonyl peak (the peak that was not hydrogen bonded to the surface) are plotted against elapsed time as the shear rate was increased from zero to a large value and then returned to zero. At each shear rate 1 h was allowed for equilibration.

First, we consider adsorption from stagnant solution. During the initial hour shown in Figure 4 (this was the final stage of adsorption from stagnant conditions), $A_x = A_y$, and A_z was slightly less, as noted in the previous section. To interpret this, first we note that molecular models show that the C═O bond has an angle of 55° relative to the PMMA chain backbone. Because it can rotate freely around the backbone, the average dipole is largest in this direction—it tends to be in an orientation that is closer to perpendicular than parallel to the backbone. Previous studies of PMMA adsorption onto oxidized silicon from stagnant solution showed the C═O peak to be preferentially vertical, relative to the surface at low surface coverage,[23] indicating that the polymer chains were relatively flattened. The molecular weight in the present experiment was much higher, however, indicating a preferentially vertical orientation of the chain backbone; therefore, it is probably reasonable to observe $A_z < A_x$. In future experiments, for more definitive interpretation it will be desirable to study polymers whose vibrational dipoles are located within the chain backbone itself.

After the onset of shear flow past the adsorbed layer, it became necessary to distinguish between changes in the free and in the bound carbonyl vibrations. For the moment, we focus on the free carbonyl. Both A_x and A_y decreased gradually with increasing shear rate, to the point that at the highest shear rate, $A_x \approx A_y \approx A_z$. There are two key observations. First, the layer showed no net alignment in the direction of shear (although there is still the possibility of some alignment of tails or some loops in this direction within the experimental error bars). Second (and the experiments are definitive on this point), the layer was compressed by the influence of shear flow by solvent.

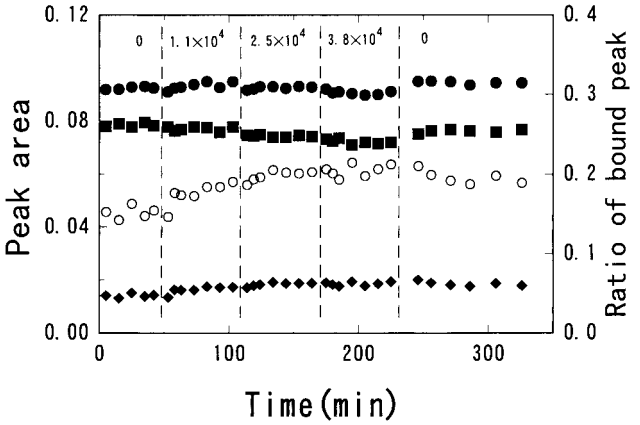

Figure 5. Plot of time evolution of the free and bound carbonyl peaks, their sum, and of the bound fraction, as PMMA adsorbed onto Ge from carbon tetrachloride solution and was exposed to solvent flow of successively larger magnitude (indicated in the figure with units of s^{-1}). The experimental conditions are the same as for Figure 4. The peak areas represent the sum of the three absorbances, A_x, A_y, and A_z. Filled squares denote free carbonyl peaks. Filled diamonds denote bound carbonyl peaks. Filled circles denote the sum of free and bound carbonyl peaks. Open circles denote the ratio of the bound to the sum of free and bound peaks. The vertical dashed lines denote times when the shear rate was changed.

Compression of the adsorbed layer by flow is also supported by the bound fraction data. Figure 5 plots the following versus elapsed time at various shear rates; the integrated areas of the free carbonyl peak, of the bound carbonyl peak, of their sum, and of the bound fraction. In stagnant solution, the adsorbed mass was ~2 mg m^{-2} with bound fraction $p \approx 0.15$, which is consistent with previous data in the literature. One observes that the total mass adsorbed scarcely changed with increasing shear rate yet that the bound mass increased while the free mass decreased. It is interesting to note that these changes took place rapidly after each step-change of shear rate (within a few minutes) except at the highest shear rate (at which the changes appeared to be more nearly continuous with elapsed time). When solvent flow was stopped after exposure to the highest shear rate, a recovery process was observed: the proportion of free carbonyl peaks increased and extra mass adsorbed, indicating readsorption of shear-detached polymer chains over a time scale of minutes.

Dependence on Shear Rate. To summarize these changes, in Figure 6 we plot the data from Figure 5 as a function of shear rate. The data were averaged after 30 min equilibration at each shear rate. One sees that the total mass adsorbed was nearly constant up to 2.5×10^4 s^{-1}; even at this high shear rate, desorption was minimal. It is true that earlier work with polystyrene had observed some desorption at lower shear rate.[9] The molecular weight of the PMMA in the present study was somewhat smaller, however. Further, the segmental sticking energy of PMMA to silicon oxide (~4 k_BT[22,23]), and therefore presumably to germanium oxide, is stronger than the sticking energy (~1 k_BT[23]) for polystyrene to silicon oxide. These considerations make it understandable that PMMA should be more difficult to desorb, although it is still a surprise that next to no desorption was observed. Even

(30) Fontana, B. J.; Thomas, J. R. *J. Phys. Chem.* **1961**, *65*, 480.
(31) Lee, J. Y.; Painter, P. C.; Coleman, M. M. *Macromolecules* **1988**, *21*, 346.

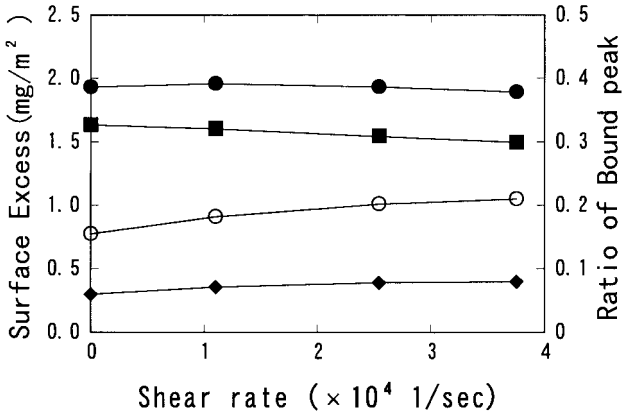

Figure 6. Surface excess and bound fraction plotted against shear rate. The experimental conditions are the same as for Figure 4. Filled squares denote free carbonyl peaks. Filled diamonds denote bound carbonyl peaks. Filled circles denote the sum of free and bound carbonyl peaks. Open circles denote the ratio of the bound to the sum of free and bound peaks.

at the highest shear rates, the desorption was less than 0.1 mg m^{-2}, i.e., only a few percent of the total adsorbed mass.

Nonetheless changes proceeded *within* the adsorbed layer. The bound mass increased with shear rate, and the free mass decreased; segments were squeezed toward the surface. The bound mass increased somewhat more rapidly than the decrease of the free mass. The observed increase of the bound fraction indicates either the increase of bound mass or the decrease of free mass. There are two possible sources for this: net flattening of the adsorbed layer (which would increase the bound mass and decrease the free mass) and desorption (which could decrease both the bound and the free mass but still affect the bound fraction because the desorbed chains can be expected to be most weakly adsorbed, i.e., to have the lowest bound fraction). At low shear rates, because the total mass remains virtually constant, we conclude that the former effect (flattening) must dominate. At the highest shear rates, the situation is more delicate, since some desorption should be expected in principle[9,10] (although the magnitude of desorption might be buried within the experimental uncertainty).

We also observed a small amount of desorption at the highest shear rate. What was the mechanism? In the simplest scenario, both the free and the bound mass would decrease upon desorption, but we did not see the latter decrease, which implies that desorption was not simply the pulling-off process of adsorbed chains. On the other hand desorption might involve more complex cooperative effects of flow and site exchange (displacement of desorbed polymer segments, accompanied by adsorption of other chains to the vacated sites). The latter scenario would be consistent with the experimental observation of no change in bound mass within the experimental uncertainty: desorption of some chains might be accompanied by a higher bound fraction of the remaining chains.

As concerns flow-induced alignment in the direction of shear flow, the data show a surprising lack of preferential alignment. In Figure 7, A_x/A_z and A_y/A_z (averaged in the same way as for Figure 6) are plotted against shear rate. The ratios concern the carbonyl group, the dipole moment of which lies preferentially normal to the backbone,[32] such that diminished A_x/A_z under flow indicates flattening. If

(32) Uemura, Y.; Stein, R. S.; MacKnight, W. J. *Macromolecules* **1971**, *4*, 490.

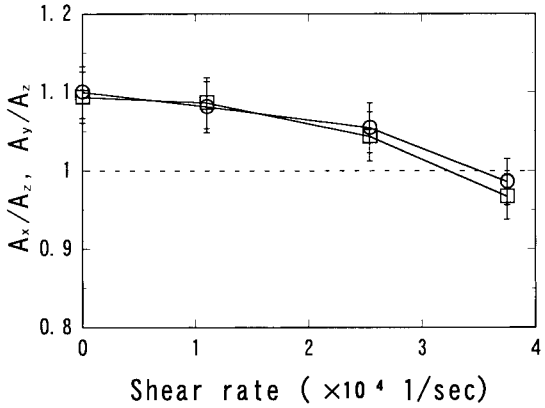

Figure 7. Infrared dichroism of adsorbed PMMA under shear flow. The experimental conditions are the same as for Figure 4. The free carbonyl peak of PMMA is shown in the *x* direction (parallel to the flow), in the *y* direction (perpendicular to the flow), and in the *z* direction (normal to the surface). The ratios A_x/A_z (circles) and A_y/A_z (squares) are also plotted against shear rate. The dashed line at the ordinate equal to unity shows the point of isotropy at which absorbance would be the same in all directions.

one wonders why $A_x/A_z \approx 1.1$ in stagnant solution, one should appreciate that this anisotropy is only slight and that an adsorbed homopolymer layer cannot be entirely isotropic.

The decrease of A_x/A_z and A_y/A_z with increasing shear rate expresses the flow compression discussed above; the observed changes in orientation relative to the normal (dichroism data) were consistent with the observed changes in the bound fraction. Within the experimental uncertainty there was no preferential alignment in the flow direction, although this observation must be qualified by recognizing that direct information about backbone alignment cannot be expected from carbonyl groups that were pendant to the backbone. For a definitive study of flow-induced backbone orientation, a polymer with an IR-active band along the backbone itself will be more suitable.

Prospects

This study was undertaken with the expectation that shear-induced desorption would be preceded, at lower shear rates than those sufficient to cause desorption, by orientation of adsorbed chains in the direction of shear flow. In hindsight, this expectation presumes that the time scale of shear flow (the inverse shear rate) exceeds the longest relaxation time of the adsorbed layer structure. The null result presented here—that $A_x = A_y$ within experimental uncertainty, despite shear-induced changes in both A_x and A_y—suggests instead the relative independence of shear-induced desorption and of relaxation times in response to deformation within the adsorbed layer. This conclusion must be considered tentative since it was not possible to study backbone orientation directly in this PMMA system. A definitive resolution of these questions must await further studies in which (a) backbone orientation can be measured directly and (b) stress at the adsorbed layer can be varied (probably by increasing the polymer concentration in solution). The experimental apparatus described in this paper will afford the experimental platform to test these questions and has already demonstrated that the adsorbed polymer layer studied here was flattened, relative to the surface, by shear flow. We also note the relevance of these question, and of the experimental approach described in this paper to related questions of wall stick or slip boundary conditions when polymer melts are caused to flow past surfaces.

Acknowledgment. We thank Dr. Peter Frantz, Dr. Erwin P. Enriquez, and Mr. Everett Geizer (machine shop, University of Illinois) for contributions to this work. Support was provided by the National Science Foundation (Tribology Program) and by the Air Force Office of Scientific Research. I.S. also thanks the Mitsubishi Chemical Corporation for financial support and for the opportunity to carry out this work.

LA9800405